Flux and Structures in Fluids, 11 th Session, Moscow, 20-22 June 2001.

NONLINEAR GEOSTROPHIC ADJUSTMENT OF DENSITY FRONT

A. Stegner (1), P. Bouruet-Aubertot (2), T. Pichon (3)

(1) Laboratoire de Météorologie Dynamique , IPSL, ENS,
24 Rue Lhomond, 75005 Paris, France. Email: stegner@lmd.ens.fr
(2) LODYC,IPSL, Universite Pierre et Marie Curie,
Jussieu, 75252 Paris Cedex 05, France.
(3) UME , ENSTA Centre de l'Yvette,
Chemin de la huniere, 91120 Palaiseau Cedex, France.

This study deals with the non-linear cyclo-geostrophic adjustment of a circular density front in a two-layer stratified fluid. Laboratory experiments and numerical simulations have been performed to investigate the dynamical evolution of a fixed volume of fresh water, initially confined within a cylinder, which is quickly released in a dense rotating fluid. This configuration corresponds to a rapid input of potential energy in a geostrophic fluid layer and reproduce some dynamical processes which occur during oceanic upwelling or stratospheric warming events. The mean adjusted state observed in laboratory is relatively well predicted by standard adjustment theory based on lagrangian conservation of potential vorticity. However, strong three-dimensional motions (plume structures and shocks) in the early stage of adjustment affects the frontal region where the density interface intersects the free surface. During the adjustment, an important part of the initial potential energy is transfered to inertia-gravity waves modes. Theses modes exhibit a non-trivial structure where the kinetic energy fluctuations are concentrated in the frontal region while significant potential energy fluctuations may occur in the central region. For all cases studied, the deviation of the density interface first oscillate at the inertial frequency. Hence, the energy released to the wave modes during the adjustment is mainly concentrated at the inertial frequency. Afterwards, frequency doubling could occur for large amplitude waves.

1. Introduction

The geostrophic adjustment is the first dynamical process which convert a significant fraction of the potential energy input (thermal or density source) of the atmosphere and the ocean into kinetic energy. During the rapid adjustment toward a quasi-equilibrium state an important part of the initial energy could be transfered to inertia-gravity waves or dissipated through small-scale three dimensional motions. Theses transient dynamical events play an important role in the inertia-gravity wave emission and local mixing in the vicinity of atmospheric jets and oceanic currents.

The first theoretical guidelines to solve geostrophic adjustment problems were proposed by Rossby (1938) and Obukhov (1949) in the framework of rotating shallow-water fluid. They assume that any initial unbalanced state, will evolve naturally toward a steady balance state, geostrophic or cyclo-geostrophic, satisfying mass and lagrangian conservation of potential vorticity (PV hereafter). This approach conveniently avoid the time-dependent problem, and gives a prediction for the final state. However, the final energy of the predicted adjusted state is less than the initial energy. Inertia-gravity waves, with zero potential vorticity, are expected to carry the missing part of the initial energy away from the adjusted state.

Nevertheless, this standard approach gives no information on the spatial and the temporal structure of the inertia-gravity wave emitted. Besides, irreversible interactions between the waves and the mean adjusted flow, and small-scale dissipative processes could strongly modify this classical scenario of geostrophic adjustment.

In this paper, we report on a laboratory experiments and numerical simulations designed to study the non-linear adjustment of a localised density anomaly in a rotating environment. A fixed volume of fresh water, initially confined within a cylinder, is quickly released in a dense fluid. Similar experiments (Griffiths & Linden, 1981; Bouruet-Aubertot & Linden, 2001) were performed to study the baroclinic instability of a density front leading to meander and eddies. The present experiment was made in a different range of parameters in order to study in detail the initial stage of adjustment. Using a non-intrusive visualisation technique, for the laboratory experiment, we were able to follow the vertical cross section of the density interface. We focus our work on: the intermediate stages of adjustment, a detailed comparison of the mean state with the adjusted state predicted by standard adjustment theory and the spatio-temporal evolution of inertia-gravity oscillating modes trapped inside the density anomaly.

2. Experimental setup and dimensionless parameters

The experiments were conducted on a 1.5 m diameter rotating turntable at the department of mechanics UME, ENSTA Palaiseau. The upper plate of this turntable rotates on a thin air layer to reduce friction and avoid all mechanical vibrations around the inertial frequency. We used a rectangular tank 48 cm large (L=24 cm), 130 cm long and the working depth H was varied from 14 cm to 30 cm.

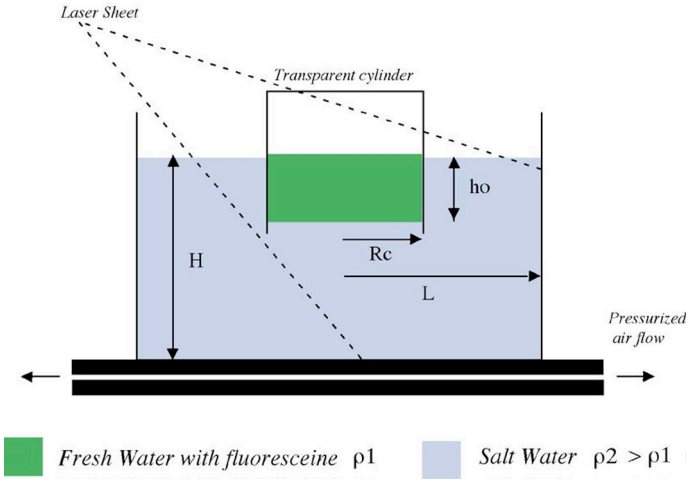

Fig.1 Sketch of the experimental apparatus

A cylindrical patch of fresh water is initially confined within a transparent bottomless cylinder. We used two cylinders of radius Rc 3.45 cm and 5.25 cm and the initial thickness ho of this density anomaly was varied from 1cm to 4cm. The salinity of the lower layer was varied from 5g.l-1 to 40g.l-1.

In order to visualise a vertical cross section of the density anomaly, the fresh water was uniformly dyed with fluoresceine and lightened from above with a vertical laser sheet (fig.1). A CCD camera, fixed on the side of the tank, perpendicular to the laser sheet, was directly connected to a computer system with a frame-grabber card and the image processing software NIH Image[1]. With this original non-intrusive technique we were able to measure the displacement of the interface between the fresh and dense water with an accuracy of 0.2 mm at the acquisition rate of 25Hz.

After the withdrawal of the cylinder, the dynamical evolution of the density anomaly is mainly governed by three dimensionless parameters, the Burger number Bu, the vertical aspect ratio δ and the front steepness ε:

$$Bu = \left(\frac{R_d}{R_c}\right)^2, \qquad \delta = \frac{h_o}{H}, \qquad \varepsilon = \frac{h_o}{R_d}$$

where $R_d = \sqrt{g^* h_o}\,/2\Omega_o$ is the deformation radius and $g^* = \frac{\Delta\rho}{\rho} g$ the reduce gravity.

In order to focus our study on the geostrophic adjustment it was needed to avoid or reduce the growth of baroclinic unstable modes which could rapidly break the adjusted state (Griffiths & Linden, 1981; Bouruet-Aubertot & Linden, 2001). Therefore, we restrict our experiment to small aspect ratio only δ~0.08-0.1, while the Burger number and the front steepness were varied in the following range of values: Bu~0.08-1.5, ε~0.4-1.2.

3. Numerical model

The primitive equation model OPA (Madec et al., 1998) is implemented in a configuration as close as possible to the experimental one (Fig.1). The hydrostatic primitive equations are discretized on a Cartesian grid such that the resolution is the same in the x and y horizontal directions, equal to 0.25cm. Vertical depth levels are chosen according to the initial stratification : the spacing between depth levels, Δz, increases from 1.5mm at small depths up to 2cm close to the bottom.

Dissipation is modeled for the horizontal velocity components using a biharmonic operator for the horizontal derivatives and a harmonic operator for the vertical derivatives. In addition a non penetrative convective adjustment algorithm is used when static instabilities arise (e.g. Madec et al, 1991). The Prandtl number Pr=ν/κ is equal to 1 so that the diffusivity κ is equal to ν. Lateral boundary condition for the horizontal velocity is no-slip and the friction at the bottom boundary is linear, for consistency with the laboratory experiments.

[1] Free software developed at the U.S. National Institutes of Health, available at http://rsb.info.nih.gov/nih-image/

4. Stages of geostrophic adjustment

Three stages in the geostrophic adjustment of the density anomaly were observed. Just after the rapid withdrawal of the transparent cylinder, the fresh water spread radially and exhibits typical features of gravity current (fig.2.a). During this first initial stage, the flow is fully three dimensional and the effects of rotation are expected to be weak. After approximately half the inertial period Tf=□/□o, the radial extension of the density front is stopped and a strong reverse flow appears. This second stage corresponds to a radial contraction of the density anomaly. During this contraction, steep jumps in the interface (analogous in their shape to hydraulic jump or shock) may appear (fig.2.b). After one or two inertial period Tf, the density front reaches an equilibrium. Standing wave mode of oscillation appears around a mean state (fig.2.c and 2.d). The amplitude of these oscillating modes could be small or large depending on the initial state.

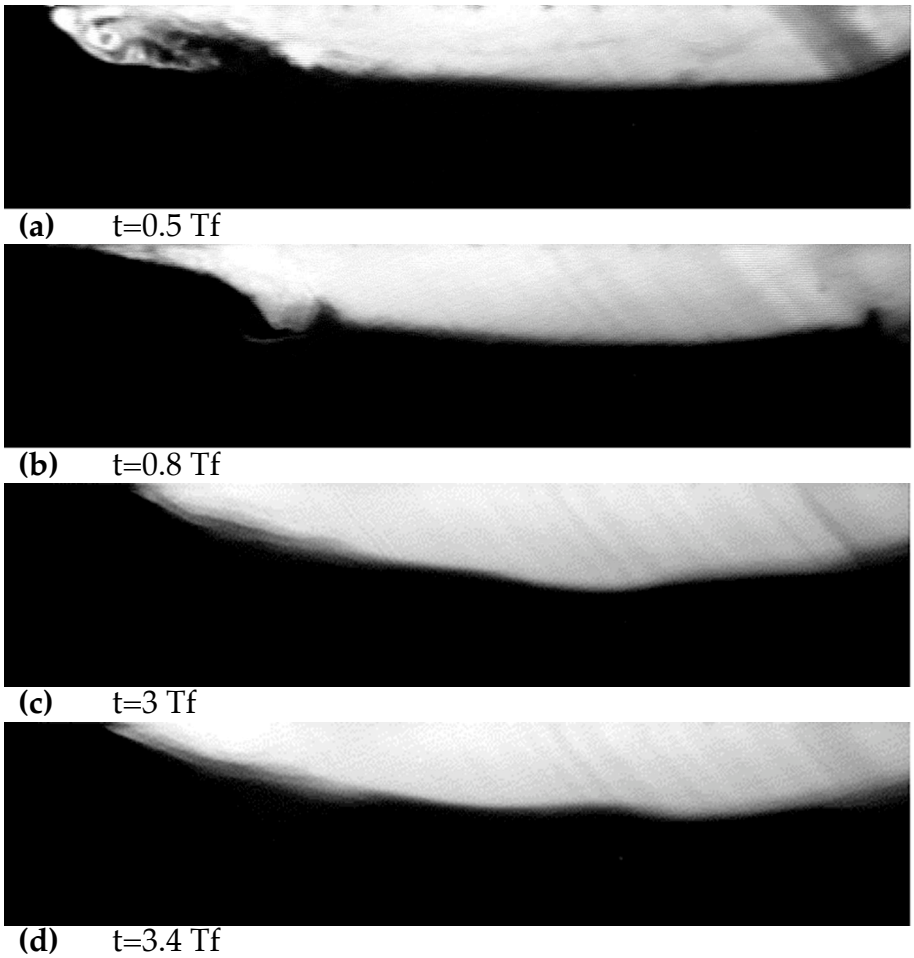

Fig.2 Dynamical evolution of the density anomaly (vertical cross section) corresponding to ho=2.5cm, Rc=5.25 cm, H=30cm, □o=0.96 rad.s-1 and □□/□=0.016. Fresh water is white due to the fluorescent light emission and dense water is black. The dark rays on the right of figs are experimental shadows.

The characteristic time of the two first stages described above does not depend on the Burger number Bu or the front steepness □. In all our experiments, the third stage, corresponding to a mean adjusted state coupled with standing oscillating modes, is rapidly reached after approximately one or two inertial periods of rotation. Theses results agree with Mahalov & al. (2000) who also found that the inertial period Tf is the characteristic transition time of bottom density current to a geostrophic front.

Note that, in the present experiment the interface between the two fluids intersect the free surface. Hence, unlike the standard Rossby adjustment problem (Gill, 1982) inertia-gravity wave cannot propagate away from the region of initial density anomaly. However, using time averaging, we can easily separate, during the third stage, the slow dynamics of the mean profile and the fast dynamics of the oscillating modes.

5. Mean adjusted state

The evolution of the mean profile, averaged over one inertial period Tf=□/□o, is shown in figure.3. This temporal averaging filters out the fast dynamics and especially the spatial structure of the inertial standing wave modes (see fig.2.c and 2.d). As it is shown in figure.3 the thickness of the density anomaly and the steepness of the front slightly decay in the laboratory experiment from 2Tf to 9Tf. This evolution corresponds to a slow radial spreading of the lens. The characteristic time of this spreading is always one or two order of magnitude higher than the inertial period. Hence, even if a perfect steady state cannot be obtained due to the Ekman decay or the horizontal viscous dissipation, the mean profile of the mass anomaly reaches a quasi-equilibrium state. Therefore, the first averaged profile (at 2Tf or 3Tf for instance) will be identified as the mean adjusted profile in the following paragraphs.

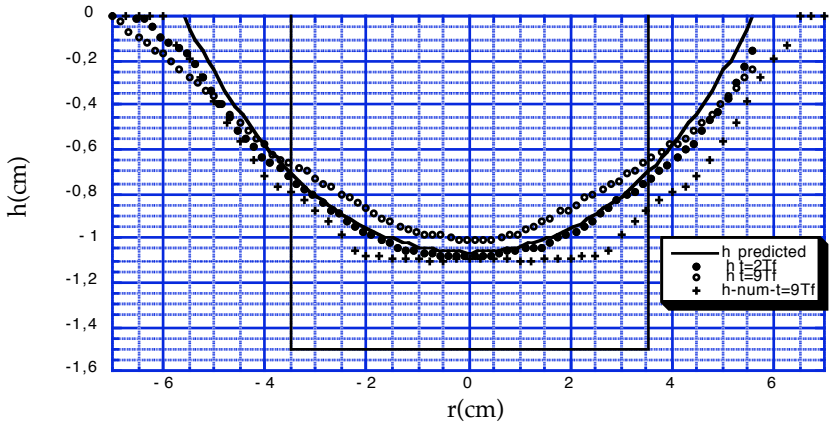

Fig.3 Mean density interface, averaged over Tf, for ho=1.55cm, Rc=3.45 cm, H=20cm, □o=1.047 rad.s-1 and □□/□=0.015 (Bu=0.33; □=0.08; □=0.76). Initial mass anomaly: fine solid line; averaged profile at t=2Tf: black dots; at t=9 Tf open dots; numerical simulation at t=9Tf :crosses ; profile predicted by standard adjustment theory: thick solid line.

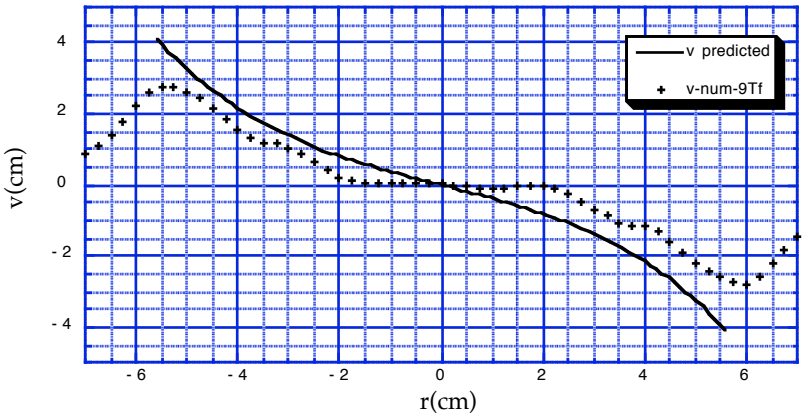

Fig.4 Azimuthal velocity after adjustment for the same initial parameter than fig.3. Numerical simulation: crosses; velocity predicted by standard adjustment theory: thick solid line.

The adjusted solution corresponding to an initial cylindrical mass anomaly was first calculated by Csanady (1979) for the geostrophic equilibrium and Flierl (1979) for the cyclo-geostrophic equilibrium. Theses solutions were obtained in the framework of the 1-1/2 shallow-water model neglecting the motion in the deep lower layer. This assumption is reasonable in our case because the vertical aspect ratio □~0.08-0.1 is small for all experiments. The shape of thus adjusted state, calculated according to the standard adjustment theory (i.e. mass conservation and lagrangian PV conservation), depends only on the Burger number Bu.

The predicted height and velocity profiles of a cyclo-geostrophic lens corresponding to Bu=0.33 are plotted (thick solid line) on figures 3 and 4. The analytical solution fits correctly the mean adjusted density profile (measured at 2Tf) in the central region while, an systematic deviation appears in the frontal region where the density interface intersect the free surface. In this region, strong mixing and three dimensional motion occurs during the very first stages of adjustment (see fig.2.a & 2.b), besides in the later stage (t>2Tf) internal wave breaking could occur where the lens thickness tends to zero. Therefore, it is not surprising to observe in the experiment a systematic radial extension of the density front. Both, the steepness of the front and the maximum azimuthal velocity (figure.4) are over-

estimated by the standard inviscid adjustment model. To quantify the accuracy of the adjustment model for various values of the Burger number, we use two dimensionless lengths that characterise the shape of the mean adjusted profile. The first one is the ratio h/h0 in the centre of the lens, where h is the mean thickness of the adjusted profile at r=0 and h0 the initial thickness of the density anomaly. The second one is the relative front displacement d/Rd, where d=Rf-Rc is the difference between the radius of the adjusted lens Rf and Rc the initial radius of the density anomaly. According to figure 5, the thickness of the adjusted lens is well predicted by the standard adjustment (5.a) while, the radial extension of the front is under-estimated by the inviscid model (5.b).

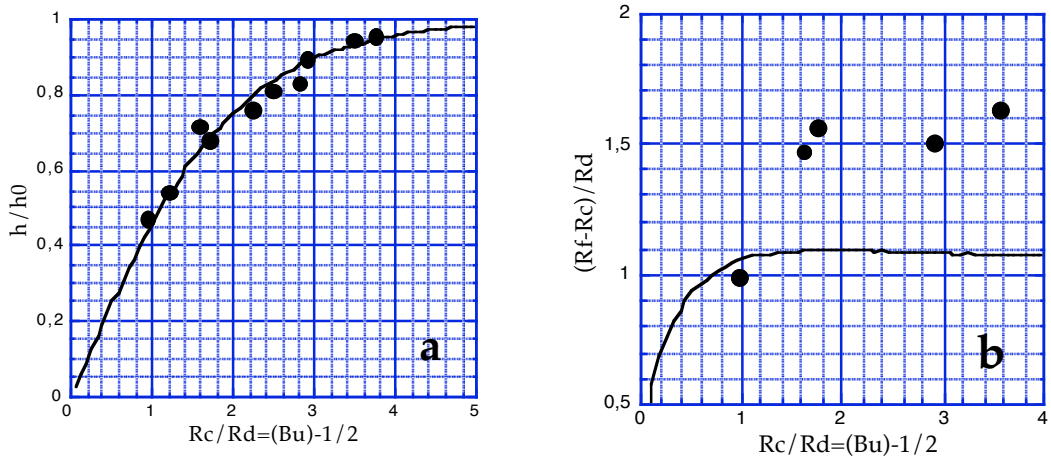

Fig.5 Thickness of the density anomaly in the centre h(r=0) (a) and relative front displacement d/Rd=(Rf-Rc)/Rd (b) after adjustment (t=2Tf) for various values of Rc/Rd=(Bu)-1/2. Experimental results: black dots; standard adjustment theory: thick solid line.

6. Fast inertial modes of oscillation

Superimposed to the mean adjusted profile, we observe standing modes having a short period of oscillation (see for instance fig.2c & 2.d). A typical structure of theses oscillations is shown in figure 6. Finite amplitude deformation may appear in the central region, while the density interface in the frontal region will remain almost unperturbed. On the other hand, the velocity field fluctuation (obtained in numerical simulation) is maximal in the frontal region, and may even extend outside the density anomaly, see for instance figure.7 at r=8 cm (density front at r=6-7 cm according to fig.3).

For all the experiments, just after adjustment, the density interface oscillates almost at the inertial period (figure 9.a). Surprisingly, this frequency remains constant while the burger number was varied from 0.08 to 1.5. In the present case, unlike classical inertial plane waves, significant vertical oscillation of the density interface can be observed at the inertial frequency. This is mainly due to the negative vorticity of the mean flow □ in the centre which reduce the effective coriolis parameter feff=2□o+□. If □<0 is of the same order of magnitude than f, velocity and height fluctuations could have similar amplitude.

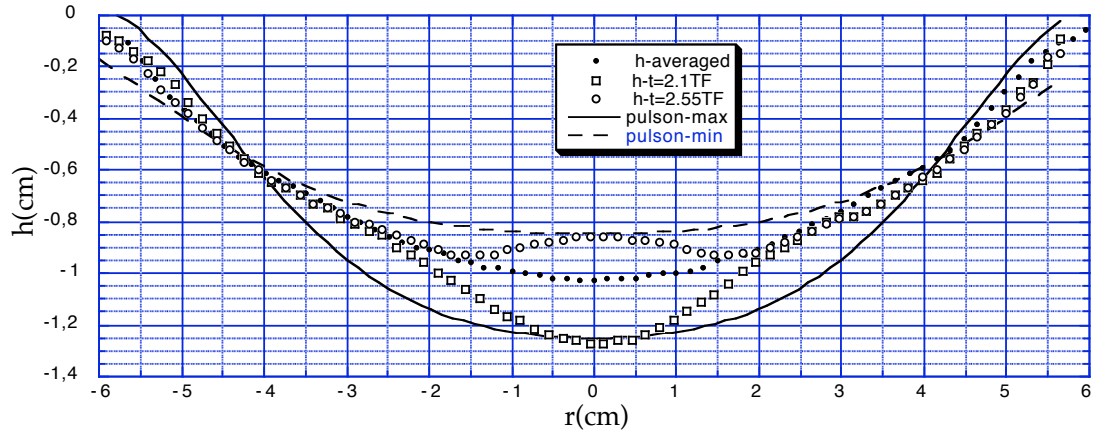

Fig.6 Fast oscillation of the density interface after adjustment for Bu=0.33; □=0.08; □=0.76. Average profile over Tf: black square; interface at t=2.1 Tf; open square; at t=2.55Tf open circle. Profiles of an oscillating pulson (according to Rubino & *al.* 1998) having the same amplitude in the center r=0: solid and dashed lines.

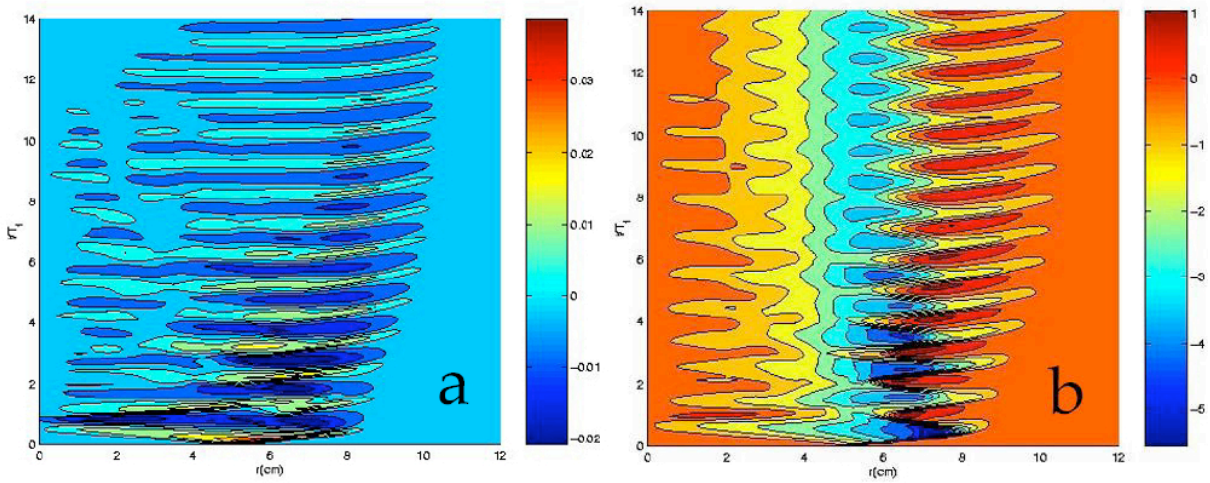

Fig.7 Spatio-temporal fluctuations of radial (a) and azimuthal (b) velocity obtained in numerical simulation with Bu=0.33, □=0.08 and □=0.76. Vertical axis: dimensionless time t/Tf; horizontal axis: radius in cm; color table: velocity amplitude in cm.s-1.

Recently, non-linear analytical solution of frontal warm-core eddies for shallow-water equations, oscillating exactly at the inertial period were found (Cushman-Roisin, 1987; Rubino & al., 1998). Therefore, we made a detailed comparison of the so-called pulson solutions with the experimental observations. The mean density profile (black square fig.6) was fitted with an eight-order polynomial. Using the polynomial fit and the amplitude of oscillation, measured in the centre, we construct the corresponding pulson solution according to Rubino & al. (1998). The extremal profiles of this solution (at t=Tf/4 and t=3Tf/4) are plotted with solid and dashed lines in fig.6. The spatial structure of the inertial standing mode observed in the experiment differs from the pulson solution. This later corresponds to a global oscillation of the density profile, unlike the observed standing mode.

If we look in more detail at the temporal evolution of the density interface in the centre we noticed two different behaviours. When the relative amplitude of oscillation is small, the inertial pulsation exhibits a long time envelope (fig.8.a). This envelope is characteristic of a slow modulation and differs strongly from an exponential decay (usually found for linear dissipation process) or the constant amplitude pulson solution. Similar modulations were also found in the numerical simulations and the previous DNS of Verzicco & *al.* 1997.

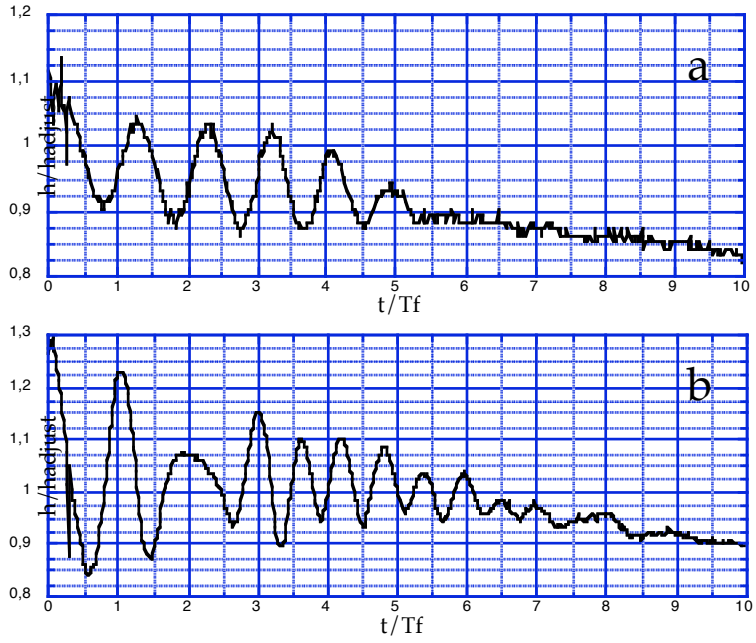

Fig.8 Oscillations of the density interface in the centre for two different set of parameters: Bu=0.18 (a), Bu=0.38 (b) while □=0.08 and □=0.8.Vertical axis: relative amplitude h(r=0)/hadjust, where hadjust is the mean thickness in the centre; horizontal axis: dimensionless time t/Tf.

However, when the relative amplitude of oscillation is large, frequency doubling appears. The two or three first oscillations are close to the inertial period, then the period is suddenly reduced (fig.8.b). A detailed analysis of this bifurcation shows that for large relative amplitude, this second pulsation reaches a value equal to twice the inertial frequency. This frequency doubling occurs when the relative amplitude of oscillation in the center exceed a critical value around 0.14-0.18 (fig.9.a).

In the same time, we have noticed that the relative amplitude of the inertial oscillation affects strongly their lifetime. For the weak amplitude regime, when the density interface oscillates only at the inertial period, their characteristic life time Tlife can be easily measured: for instance Tlife=5.5Tf in fig.8.a . As it is shown in figure 9.b, the lifetime of the inertial trapped modes tends to decrease when their relative amplitude increases. This tendency cannot be explained by classical Eckman damping or any linear dissipative processes. The lifetime of inertial modes localized in theses adjusted density fronts is then probably governed by a non-linear dissipation. The local Froude number increases dramatically in the frontal region where the density interface intersect the free surface (i.e. when the thickness tends to zero). Hence, all wave motions will be affected by non-linear steepnening and

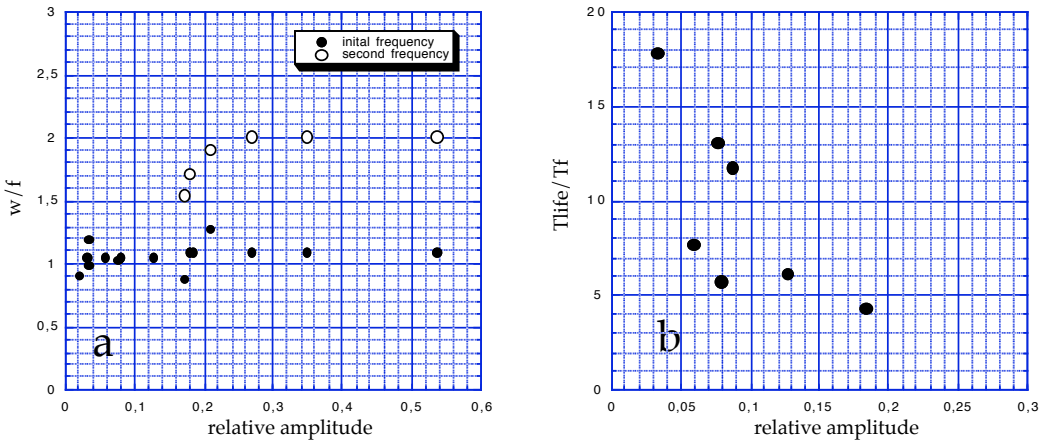

breaking process in this region.

Fig.9 Frequency of the oscillation (a) in the middle of the lense and lifetime of the inertial oscillation (b) as a function of the maximum value of the relative amplitude. Black dots corresponds to the first oscillation just after adjustment, open dots corresponds to the frequency measured after the frequency bifurcation.

7. Conclusion

By the mean of laboratory experiments and numerical simulations, we have examined, in a wide range of parameter, the non-linear adjustment of density front and the resulting inertial wave motion.

The mean adjusted state observed in laboratory is relatively well predicted by standard adjustment theory. However, strong three-dimensional motions (plume structures and shocks) in the early stage of the adjustment affect the frontal region where the density interface intersects the free surface. In this region, the predicted state contains an unrealistic velocity discontinuity. Therefore, local dissipation tends to increase the radial propagation of the density front, during the adjustment, and to reduce the maximum velocity of the cyclo-geostrophic jet.

The mean adjusted state appears after one or two inertial periods. Afterwards, standing inertia-gravity wave modes are trapped inside the density anomaly. Theses modes exhibit a non-trivial structure where the kinetic energy fluctuations are concentrated in the frontal region while significant potential energy fluctuations may occur in the region of constant PV

The temporal behaviour of these modes is striking. For all the case studied, the oscillations first occur at the inertial frequency. In other words, the energy transfered during the adjustment to inertia-gravity wave motion is mainly concentrated at the inertial frequency. Besides, both weak and strong amplitude oscillations are affected by non-linear processes. On one hand, frequency doubling appears when the relative amplitude exceeds a critical value. On the other hand, the lifetime of weak amplitude mode is inversely proportional to its amplitude. Therefore, theses modes seem to be controlled by a non-linear dissipation such as local wave breaking in the frontal region.

Acknowledgements: We gratefully acknowledge V. Zeitlin for enlightening discussions, Gregoire Jourdan and Jean Noel Vidal for their valuable contribution to the experiment and J.P. Larue for his technical support. This work was supported by the ACI “jeunes chercheurs” CNRS n° 0693. The numerical simulation were performed on the NEC SX-5 of the Institut du Developpement et des Ressources en Informatique Scientifique (IDRIS) under contract 011396.

References :

Bouruet-Aubertot, P., Linden, P.F. PartI: Laboratory experiments on upwelling fronts: the influence of the coast. *Submitted to Dyn. Atmos. Ocean* , 2001.

Bouruet-Aubertot, P. , Echevin, V. The influence of the coast on the dynamics of upwelling fronts. the influence of the coast. Part II : Numerical simulations . *Submitted to Dyn. Atmos. Ocean* , 2001.

Csanady, G.T. 1979 The birth and death of a warm core ring, *J. Geophys. Res.* v. 82, 777-780.

Cushman-Roisin, B. 1987 Exact analytical solution for elliptical vortices of the shallow-water equations. *Tellus*, 39A, 235-244.

Flierl, G.R. 1979 A simple model for the structure of warm cold core rings, *J. Geophys. Res.* v. 82, 781-785.

Gill, E. 1982 Atmosphere-Ocean Dynamics, 662 pp. *Academic Press, Inc. London.*

Griffiths, R.W., Linden, P.F. 1981 The stability of vortices in a rotating, stratified fluid. *J. Fluid Mech.*, v.105, 283-316.

Madec, G., Delecluse, P., Imbard, M., Levy, C. 1998. OPA8.1 ocean general circulation model reference manual, Institut Pierre Simon Laplace, note 11, 91pp. available at http://www.lodyc.fr/opa/

Madec, G., Chartier, M., Delecluse, P., Crépon, M. 1991 A three-dimensional numerical study of deep water formation in the Northwestern Mediterranean Sea *J. Phys. Oceanogr.*, 21, 1349-1371.

Mahalov, A. & *al*. 2000 Effects of rotation on fronts of density currents. *Phys. Lett. A* 270, 149-156.

Obukhov, A.M. 1949 On the question of the geostrophic wind. *Izv. Akad. Nauk SSSR, Ser. Geogr. Geofiz.* v.13 , 281.

Rossby, C.G. 1938 On the mutual adjustment of pressure and velocity distribution in certain simple current systems II. *J. Mar. Res.* v.1, 239-263.

Rubino, A. & al. 1998 Analytical solutions for circular eddies of the reduced-gravity shallow-water equations. *J. Phys. Oceanography* v.28, 999-1002.

Verzicco, R. & al. 1997 Dynamics of baroclinic vortices in a rotating, stratified fluid: a numerical study. *Phys. Fluids* 9 (2), 419-432.